The Astrophysical Journal, 878:58 (7pp), 2019 June 10 https://doi.org/10.3847/1538-4357/ab1e4d

The Fate of Binaries in the Galactic Center: The Mundane and the Exotic

Alexander P. Stephan[1,2], Smadar Naoz[1,2], Andrea M. Ghez[1], Mark R. Morris[1], Anna Ciurlo[1], Tuan Do[1], Katelyn Breivik[3], Scott Coughlin[4,5], and Carl L. Rodriguez[6,7]

[1] Department of Physics and Astronomy, University of California, Los Angeles, Los Angeles, CA 90095, USA; alexpstephan@astro.ucla.edu
[2] Mani L. Bhaumik Institute for Theoretical Physics, University of California, Los Angeles, Los Angeles, CA 90095, USA
[3] Canadian Institute for Theoretical Astrophysics, University of Toronto, 60 St. George Street, ON M5S 3H8, Canada
[4] Physics and Astronomy, Cardiff University, Cardiff, CF10 2FH, UK
[5] Center for Interdisciplinary Exploration & Research in Astrophysics (CIERA), Northwestern University, Evanston, IL 60208, USA
[6] MIT-Kavli Institute for Astrophysics and Space Research, 77 Massachusetts Avenue, 37-664H, Cambridge, MA 02139, USA
Received 2019 February 28; revised 2019 April 17; accepted 2019 April 29; published 2019 June 13

Abstract

The Galactic center is dominated by the gravity of a super-massive black hole (SMBH), Sagittarius A*, and is suspected to contain a sizable population of binary stars. Such binaries form hierarchical triples with the SMBH, undergoing Eccentric Kozai–Lidov (EKL) evolution, which can lead to high-eccentricity excitations for the binary companions' mutual orbit. This effect can lead to stellar collisions or Roche-lobe crossings, as well as orbital shrinking due to tidal dissipation. In this work we investigate the dynamical and stellar evolution of such binary systems, especially with regards to the binaries' post-main-sequence evolution. We find that the majority of binaries ($\sim$75%) is eventually separated into single stars, while the remaining binaries ($\sim$25%) undergo phases of common-envelope evolution and/or stellar mergers. These objects can produce a number of different exotic outcomes, including rejuvenated stars, G2-like infrared-excess objects, stripped giant stars, Type Ia supernovae (SNe), cataclysmic variables, symbiotic binaries, or compact object binaries. We estimate that, within a sphere of 250 Mpc radius, about 7.5–15 SNe Ia per year should occur in galactic nuclei due to this mechanism, potentially detectable by the Zwicky Transient Facility and ASAS-SN. Likewise, we estimate that, within a sphere of 1 Gpc^3 volume, about 10–20 compact object binaries form per year that could become gravitational wave sources. Based on results of EKL-driven compact object binary mergers in galactic nuclei by Hoang et al., this compact object binary formation rate translates to about 15–30 events per year that are detectable by Advanced LIGO.

Key words: binaries: general – Galaxy: center – novae, cataclysmic variables – stars: black holes – stars: evolution – stars: kinematics and dynamics

1. Introduction

The Galactic center (GC) contains the closest known super-massive black hole (SMBH), Sagittarius A*, which dominates the gravitational dynamics of its environment due to its large mass of about $4 \times 10^6\,M_\odot$ (e.g., Ghez et al. 2005; Gillessen et al. 2009). Thus, the environment of the GC has served as a "laboratory" to test the nature of gravity, stellar cluster dynamics, and general relativity (GR) over the last decades (e.g., Ghez et al. 2003, 2005; Alexander 2005; Hopman & Alexander 2006; Gillessen et al. 2009, 2012; Hopman 2009; Alexander & Pfuhl 2014; Hees et al. 2017; Chu et al. 2018). The gravitational influence of the SMBH is suspected to cause a number of interesting astrophysical phenomena, such as hypervelocity stars (e.g., Ginsburg & Loeb 2007) and stellar binary mergers (e.g., Antonini et al. 2010, 2011; Prodan et al. 2015; Stephan et al. 2016). Furthermore, there appears to be a large number of X-ray sources associated with the GC, sometimes interpreted to indicate a large number of X-ray binaries, stellar-mass black hole–star binary pairs, where the black hole accretes material from its companion, emitting X-ray radiation (e.g., Muno et al. 2005; Cheng et al. 2018; Zhu et al. 2018). Muno et al. (2006, 2009) and Heinke et al. (2008), however, suggested that many of the observed GC X-ray sources are actually cataclysmic variables (CVs), consisting of white dwarf (WD)–main-sequence star binary pairs.

Any binary that orbits the GC's SMBH will feel gravitational perturbations on the binary's orbit by the SMBH. These perturbations can lead to chaotic orbital eccentricity and inclination excitations, the so-called Eccentric Kozai–Lidov (EKL) mechanism (see, for a review, Naoz 2016). This effect can cause binary stars in the GC to merge (e.g., Antonini et al. 2010, 2011; Antonini & Perets 2012; Witzel et al. 2014, 2017; Prodan et al. 2015; Stephan et al. 2016; Fragione 2019), which has been used to explain extended infrared-excess objects such as G2 (e.g., Gillessen et al. 2012). However, the exact nature of these merger-candidate events is not always the same. While some binary stars might just collide or have grazing encounters due to the induced large eccentricities, others might first undergo orbit shrinking and circularization due to tidal dissipation, and might not begin merging until the stars begin to expand due to stellar evolution (Stephan et al. 2016). The shrinking of the orbit can furthermore "harden" the orbit and make it long-term stable against scattering interactions with other stars in the GC (compare also with Trani et al. 2019), allowing the binary companions to remain coupled long enough for the stars to leave the main sequence and become red giants.

In this work, we investigate the possible outcomes of post-main-sequence binary star evolution in the GC, taking into consideration the effects of EKL, tides, GR, and interactions with the GC's stellar cluster. Most of these stars end their regular lives as WDs ($M_{*,\mathrm{ini}} \lesssim 8\,M_\odot$), as these constitute the bulk of the stellar population (e.g., Salpeter 1955), and which could serve as progenitors of Type Ia supernovae (SNe).

[7] Pappalardo Fellow.

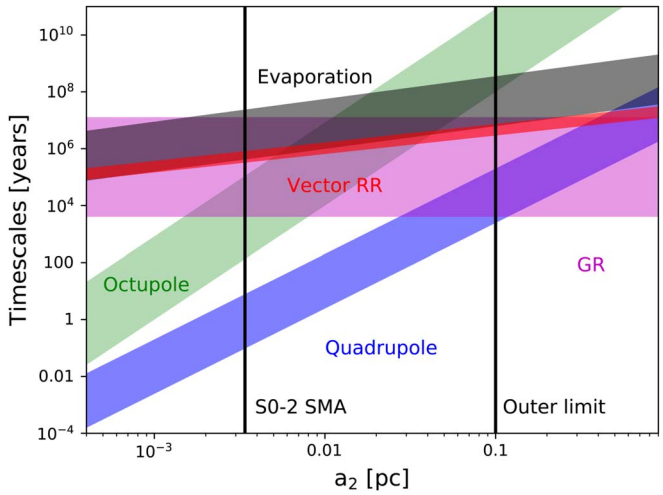

Figure 1. Timescales of physical effects in the GC. The figure shows the timescales for several physical effects acting on binaries in the GC as a function of outer orbital distance from the SMBH, such as GR (magenta), vector resonant relaxation (red), evaporation (dark gray), and the timescales for the quadrupole (blue) and octupole (green) levels of the EKL mechanism. The filled areas show the strengths of these effects for a range of possible binary parameters, ranging in combined binary mass from 2 to 10 $M_\odot$ and in binary semimajor axis from 1 to 10 au. The black lines show the inner and outer limits of semimajor axis (SMA) values around the SMBH used in this work, from ~700 au to 0.1 pc.

Furthermore, we also consider progenitors of stellar-mass black holes and neutron stars.

2. Numerical Setup

In Stephan et al. (2016), we executed a large Monte Carlo simulation of binary stars in the inner 0.1 pc around the GC's SMBH that explored the dynamical evolution of the binaries until they either merged, tidally locked, or separated. In this work, we expand on these earlier simulations and use the same system parameters for our new Monte Carlo runs: the primary stellar mass was chosen from a Salpeter distribution with $\alpha = 2.35$ (Salpeter 1955), with the masses limited between 1 and 150 $M_\odot$, the mass ratio to the secondary was taken from Duquennoy & Mayor (1991), and the mass of the SMBH was set to $4 \times 10^6 M_\odot$ (e.g., Ghez et al. 2005; Gillessen et al. 2009). The inner binary semimajor axis distribution was also taken from Duquennoy & Mayor (1991), while the outer binary semimajor axis was initially drawn uniformly between about 700 au and 0.1 pc. The inner limit corresponds approximately to the orbit of the star S0-2 (Ghez et al. 2005), while for most orbits beyond 0.1 pc the effects of vector resonant relaxation become nonnegligible (e.g., Hamers et al. 2018). This is also shown in Figure 1, where we show several important dynamical timescales for the GC. The inner binary orbit eccentricity was drawn uniformly between 0 and 1 (Raghavan et al. 2010), while the outer one was taken as thermal (Jeans 1919). The angle between the inner and outer angular momenta was drawn isotropically. These systems were then tested for orbital stability, requiring that

$$\epsilon = \frac{a_1}{a_2} \frac{e_2}{1 - e_2^2}, \quad (1)$$

where a_1 (a_2) is the inner (outer) orbit semimajor axis, and e_2 is the outer orbit eccentricity. Further analytic stability criteria had to be fulfilled, ensuring that the binaries do not cross the SMBH's tidal radius (see Naoz et al. 2016; Stephan et al. 2016, for a complete list of conditions). In total, we had 5203 stable systems, 1570 from Stephan et al. (2016) and 3633 additional ones, to provide better statistical significance. The distribution of semimajor axis and eccentricity values after application of the stability criteria for the new simulations are equivalent to the old ones shown by Stephan et al. (2016), Figure 2.

The systems were then evolved including effects from EKL, GR, tides (e.g., Naoz et al. 2016, for the complete set of equations), and stellar evolution, following the single-star stellar evolution code SSE by Hurley et al. (2000).[8] The time it takes on average for binaries to be separated by interactions with other stars in the GC, (called the "evaporation timescale") served as the time limit for our calculations. However, if tidal effects are able to shrink the inner orbital distance of a binary, its expected survival time increases, as it becomes more stable against such scattering events (for equations, see Binney & Tremaine 1987; Stephan et al. 2016). Scattering events can also lead to exchanges of stars in the binaries with other objects orbiting the GC (e.g., Trani et al. 2019); while this can have interesting implications for further secular binary evolution, the encounter and exchange rate for tidally shrunken binaries is rather low and does not substantially influence our results. Furthermore, short-period binaries do not feel strong EKL effects, as GR and tidal effects suppress the gravitational perturbations by the SMBH. This leads to the formation of a large population of long-lived short-period binaries, as described by Stephan et al. (2016) and in the present work.

High-eccentricity mergers induced by EKL occur very early in the binaries' lifetimes (as shown by Stephan et al. 2016). Radial mergers are caused by the radial expansion of one star in the binary and do not necessarily require EKL-induced eccentricity or tidal orbital shrinking (though either effect facilitates the occurrence of such mergers), and therefore occur somewhat later, when the most massive stars begin to evolve past the main-sequence. Tidal mergers are binaries that become short-period binaries due to the interplay of EKL-induced high eccentricities and tidal orbital shrinking, destined to merge during post-main-sequence stellar evolution due to stellar expansion, after hundreds of megayears or even several gigayears. Tidal mergers were the dominant merging mechanism described by Stephan et al. (2016), producing 56% of mergers, compared to 33% of mergers through EKL during the main-sequence, and 11% of mergers due to radial expansion of evolved, massive stars.

We use the merging binary systems from our simulations as the basis for this work. We take the orbital parameters of these binaries at the moment when they either crossed the Roche lobe or became tidally locked short-period binaries and determine their further binary star evolution using the binary stellar evolution code BSE (Hurley et al. 2002). In particular, we use the BSE version distributed with the COSMIC binary population synthesis suite.

Several updates have been made to the BSE version used in COSMIC. Metallicity-dependent wind prescriptions for high-mass stars have been implemented following Vink et al. (2001), Vink & de Koter (2005), and Belczynski et al. (2010). Prescriptions for compact object formation and natal kicks have

[8] It has been shown that stellar evolution can have significant effects on the dynamical evolution in many astrophysical settings involving the EKL mechanism (e.g., Shappee & Thompson 2013; Stephan et al. 2016, 2017, 2018; Petrovich & Muñoz 2017).

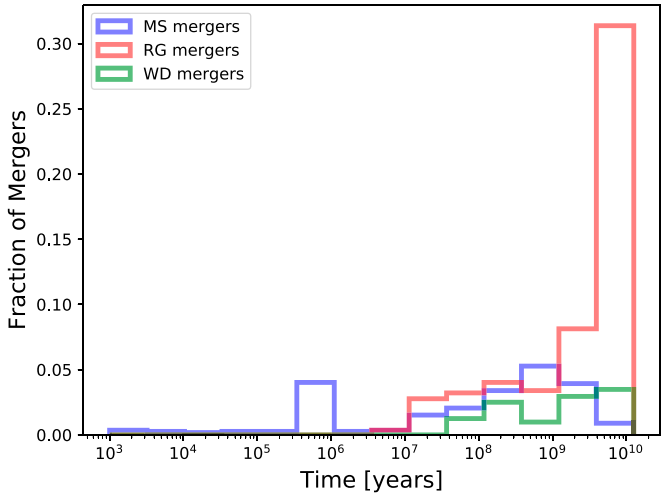

Figure 2. Types of mergers as a function of time. The plot shows a histogram of the times the main types of mergers occur. Mergers of two main-sequence stars are shown in blue, mergers involving at least one red giant star (and no WD or other compact object) are shown in red, and mergers involving at least one WD are shown in green. The peak of main-sequence binary mergers in the first megayear of evolution is due to EKL-driven high-eccentricity collisions, while the continued merging of RG and WD systems over several gigayears is due to tidally shrunken and circularized binaries. Mergers that involve at least one BH or NS constitute about 1% of the systems and are not depicted here to avoid clutter.

also been updated following Fryer & Kalogera (2001), Fryer et al. (2012), and, for electron-capture SNe for neutron stars, following Kiel et al. (2008). We used the default parameters for BSE except in the case of the updated prescriptions detailed above. In particular, we assume the "rapid" model from Fryer et al. (2012) for compact object formation and that natal kicks are drawn from a Maxwellian distribution with $\sigma = 265\,\mathrm{km\,s^{-1}}$ (Hobbs et al. 2005), with BH natal kicks being modified due to the amount of mass that falls back onto the proto-BH during formation. Finally, we note that our treatment for the common envelope follows the standard $\alpha\lambda$ formalism and default BSE values, with $\alpha = 1.0$ and λ determined by the stellar properties at the time just prior to the common envelope (Claeys et al. 2014).

BSE keeps track of the stars' evolutionary phases and, furthermore, indicates when and if binary stars merge and what type of object would be the outcome of such mergers. Double WD mergers would be candidates for SNe Ia, if their combined mass is large enough, while WD-red giant and WD-main-sequence mergers are candidates for symbiotic binaries (SBs) and CVs, as the WD would easily be able to accrete material from the companion star's envelope. Mergers involving helium stars, red giant stars, and main-sequence stars are probably candidates for G2-like objects, stars shrouded by a gaseous dust-rich cloud for a few megayears after merging had occurred (Witzel et al. 2014, 2017; Stephan et al. 2016). Helium stars themselves are examples of "stripped giants," which have been speculated to exist in the GC (Ghez et al. 2008).

We note that while we use BSE to perform the calculations for merger candidates' further stellar evolution, even for eccentric binaries, there are some limitations with this treatment (Sepinsky et al. 2007a, 2007b, 2010). However, BSE does include effects like SN kicks for neutron stars and provides results massively faster than full stellar hydrodynamic models. These are important advantages that allow us to advance this work.

3. Results and Discussion

Here we go into greater detail about the different types of outcomes and their implications for the binary population in the GC.

3.1. Dynamical Evolution Outcomes

We summarize the dynamical evolution outcomes before including binary evolution calculations below.

1. *Unbound Binaries:* 75% of the initial binary population is separated by interactions with other stars in the GC into single stars before the binary members can interact in a meaningful way. This unbinding (evaporation) of binaries begins after a few megayears of dynamical evolution and is mostly finished after a few hundred megayears (∼25% of binaries have separated after about 6 Myr). After that point, any binary that has not separated has either merged or has a tidally shrunken orbit that is long-term stable against separation.
2. *EKL Mergers:* 10% of binaries merge due to high eccentricities induced by EKL-oscillations. The binaries merge early, within the first few megayears of their dynamical evolution.
3. *Radial Mergers:* 2% of binaries merge simply due to radial expansion of one of their members during the red giant phase. These systems generally include very massive stars that evolve rapidly, within the first few megayears of evolution.
4. *Tidally Locked:* 13% of binaries have tightened and circularized their orbits due to the interplay of EKL and tides to such a degree that they are long-term stable against separation. These systems must reach this tidally locked state within only a few megayears after formation to escape evaporation. Their subsequent fate then depends on the stellar masses and orbital separation.

3.2. Binary Evolution Outcomes

The different outcomes of binary evolution are essential to understand the census of binaries in galactic nuclei. The outcomes were determined using BSE, as applied to EKL and radial mergers as well as the tidally locked binaries described above. We refer to these systems as "merger candidates." BSE evolves these systems while keeping track of common-envelope phases, Roche lobe overflow phases, mergers, kicks, and possible separation. Sometimes this will result in the formation of very tight compact object binaries instead of true mergers (e.g., Taam & Ricker 2010), though, it can usually be expected that such systems merge eventually either through gravitational wave emission or further gravitational perturbations by the SMBH. In general, the results can be divided into three groups, based on the evolutionary state of the stars when they merge:[9]

1. *Main-sequence or Red Giant Mergers:* 85.4% of merger candidates eventually merge as some combination of main-sequence, red giant, and/or helium (stripped giant) stars. We extrapolate from current observations of binary

[9] Merged stars undergo a much more violent evolution, where it can be expected that a lot of material is ejected and forms an extended envelope. Thus, while the Kelvin–Helmholtz timescale of a new star is on the order of a few 10^5 years, an extended envelope may still be engulfing it.

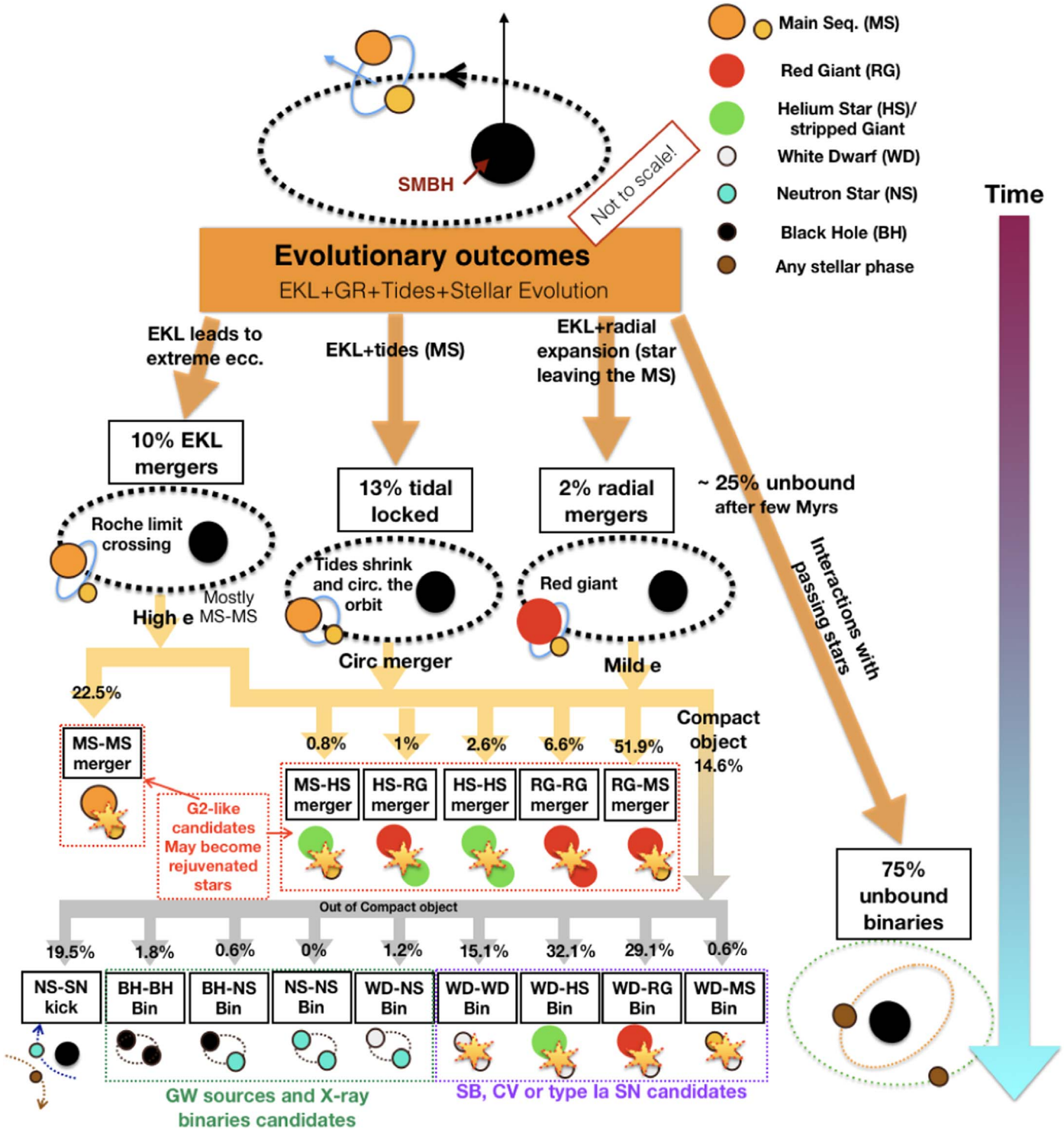

Figure 3. Flowchart of binary evolution outcomes. The diagram shows the outcomes of binary evolution in the inner 0.1 pc of the GC. Dynamical effects such as scattering with other stars separate 75% of all binaries into independent singles before they can interact with each other. 10% of binaries will collide or have grazing encounters due to EKL-induced high eccentricities. 2% will merge simply due to radial expansion of one of the binary members due to stellar evolution. 13% of binaries will tidally shrink their orbits and become decoupled from gravitational perturbations by the SMBH. We determined the further evolution of these binary pairs and their evolutionary phases during merging using BSE. The different possible outcomes are shown in the figure. Generally, the most likely combinations for merging binaries are pairs of main-sequence stars, main-sequence and red giant stars, pairs of red giant stars, and white dwarfs with evolved stellar companions. There is also a sizable population of binaries that were separated due to neutron star kicks, producing single neutron stars orbiting the SMBH, as well as a small population of binaries containing black holes or neutron stars that can become gravitational wave sources and might have been X-ray sources at some point, marked by the green box (see Bortolas et al. 2017; Hoang et al. 2018). Mergers involving white dwarfs are candidates for SBs, CVs, and SNe Ia (purple box), while mergers involving red giants, stripped giants, or main-sequence stars are candidates for G2-like objects or progenitors of rejuvenated stars (red boxes; e.g., Witzel et al. 2014, 2017; Stephan et al. 2016).

star mergers (e.g., Tylenda et al. 2011a, 2011b, 2013; Nicholls et al. 2013; Kamiński et al. 2018) that the forming objects will be shrouded by extended gas and dust clouds for an extended period of time. These mergers are therefore candidates for explaining the sizable population of observed G2-like objects (A. Ciurlo et al. 2019, in preparation). We show the occurrence rate of these mergers, split into mergers only involving main-sequence stars and mergers involving red giants, as the blue and red, respectively, histograms in Figure 2. Note that main-sequence star-only mergers tend to occur early, especially due to EKL-driven high-eccentricity mergers.

The resulting merger product may appear as a rejuvenated star, as it is now a more massive star that has burned less fuel than equally massive stars that evolved as singles. Such stars are also known as blue stragglers in open clusters (e.g., Perets & Fabrycky 2009; Geller et al. 2011; Naoz & Fabrycky 2014). The difference in measured age versus the actual age of the star could be substantial, but is highly dependent on the types of stars and their evolutionary state at the moment of merging, as well as the details of the merging process. According to the results given by BSE, the new star could appear younger by several gigayears, or just a few megayears, depending on the exact circumstances. Exploring the exact stellar evolution processes that determine the degree of rejuvenation, however, goes beyond the scope of this work. Regarding mergers involving red giants and helium stars, previous studies suggest that the resulting products can be carbon stars or even R Coronae Borealis (R CrB) variables (e.g., Iben et al. 1996; Izzard et al. 2007; Zhang & Jeffery 2013).

We note here that a small fraction of binaries can produce Type Ia-like SNe during their red giant evolution. These are mostly similar-mass stellar pairs on very short orbits ($\sim$1 day). When these binaries evolve into red giants, they form helium cores that can eventually collide as the stars enter common-envelope evolution and coalesce into a single object. As they collide, some of these helium cores are able to ignite and explode the stars without leaving a remnant behind. While this is very similar to an SN Ia, the cores' combined mass is generally very low ($\lesssim 0.5\,M_{\odot}$), probably producing somewhat less energy than a typical SN Ia ($\sim 10^{50}$–10^{51} erg; for a review of types of SNe and their luminosities, see Kasliwal 2012); such events might therefore be more difficult to identify and characterize correctly when occurring in the crowded environment of galactic nuclei. However, the combination of tidal effects and EKL with an SMBH serves to strongly enhance the formation of such short-period binaries. According to BSE, about 1% of the entire GC stellar binary population lead to such low-energy SNe.

2. *White Dwarf Binaries:* 11.2% of merger-candidate systems evolve to contain a WD star with either a WD, stripped giant, red giant, or main-sequence star companion. Such systems (i.e., WD–WD or WD–MS) are candidates for SNe Ia, given enough mass or enough collision energy. BSE evolution concluded that 15.4% of these systems would result in SNe Ia (which is 0.4% of the entire GC stellar binary population). Binaries and higher-multiplicity systems containing WDs outside of the GC have been investigated in previous studies as potential sources for WD collisions and SNe Ia, including due to EKL effects (e.g., Katz & Dong 2012; Toonen et al. 2017). The occurrence rate over time of these mergers is shown in green in Figure 2.

Given our results for SNe Ia, we can estimate the occurrence rate of such SNe in the galactic neighborhood. The GC contains on the order of $10^7\,M_{\odot}$ of stars and stellar remnants within a radius of about one parsec from the SMBH (e.g., Genzel et al. 2003; Schödel et al. 2003). Given an age of the Galaxy of about 10 Gyr, the star formation rate is approximately $10^3\,M_{\odot}\,\mathrm{Myr}^{-1}$. Assuming a Salpeter Initial Mass Function (IMF), and an average star mass of 1 $M_{\odot}$, the SN Ia likelihood is 0.4% and the SN Ia rate is $4 \times 10^{-6}\,\mathrm{yr}^{-1}$ for our GC.[10] Based on the observation statistics of the ASAS-SN collaboration (e.g., Holoien et al. 2019), we assume an effective observation radius of 250 Mpc (up to redshift 0.06), or an effectively observable sphere of 0.065 Gpc^3. Assuming a galaxy density of 0.02 Galaxies/Mpc^3 (Conselice et al. 2005), there are about 1.3×10^6 galaxies within this sphere. If we assume that half (or all) of these galaxies have central massive BHs and nuclear star clusters similar to ours, the expected rate of SNe Ia within this observable sphere would be about $2.5\,\mathrm{yr}^{-1}$ (or $5\,\mathrm{yr}^{-1}$), on average. If we also include Type Ia-like SNe from colliding helium cores (see red giant mergers), the rate is approximately tripled, to a maximum of $7.5\,\mathrm{yr}^{-1}$ (or $15\,\mathrm{yr}^{-1}$), on average; unfortunately, due to their low energy, these explosions might be more challenging to observe. However, the Zwicky Transient Facility (ZTF) should be capable of observing even these fainter supernovae, at even greater distances (Bellm et al. 2019).

Furthermore, binary pairs of WDs and main-sequence or red giant stars are also candidates for CVs or SBs, respectively, as the WDs will be accreting material from their companions for some part of their evolution. These objects, as well as some WD pairs, could remain as tight binaries for extended periods of time before merging (e.g., Taam & Ricker 2010). The large population of observed X-ray sources in the GC might be explained by these WD harboring binaries (see also Zhu et al. 2018). As the binary pairs eventually merge, some of them are candidates for carbon stars or, in some cases, R CrB variables (e.g., Iben et al. 1996; Izzard et al. 2007; Zhang & Jeffery 2013).

3. *Black holes and Neutron stars:* 3.4% of merger candidates will eventually evolve to contain a stellar-mass black hole or a neutron star, many of which could have been high-mass X-ray binaries before the secondary became a compact object; however, most of these pairs will separate due to SN kicks when the neutron stars form (see also Bortolas et al. 2017; Lu & Naoz 2019). Lu & Naoz (2019) showed that this can also bring NSs onto eccentric orbits close enough to the SMBH to merge via gravitational wave emissions, which should be detectable by LISA. Nevertheless, a small number of binary black holes and black hole–neutron star binaries will survive ($\sim$0.1% of the entire GC binary population) and can

[10] This is a conservative estimate, as the GC's actual IMF is top-heavy (Lu et al. 2013). We would expect this to lead to a higher rate than the one calculated here.

serve as gravitational wave sources in the GC (e.g., Hoang et al. 2018). The formation rate of such binaries would be about $10^{-6}\,\mathrm{yr}^{-1}$ for our GC (see calculations above for SNe Ia, assuming again a Salpeter IMF and an average star mass of $1\,M_{\odot}$). Within a sphere of 1 Gpc^3 volume, with 0.02 Galaxies/Mpc^3, and half (up to all) of galaxies containing an MBH and nuclear star cluster, the total expected formation rate of compact object binaries is about $10–20\,\mathrm{yr}^{-1}$. Assuming a merger efficiency of these compact object binaries due to further EKL effects of about 10%, as was shown by Hoang et al. (2018), this formation rate translates to about 1–2 gravitational wave signals producing inspirals per year per Gpc^3. Given Advanced LIGO's detection range of up to 1.5 Gpc (Abbott et al. 2018), this implies a rate of about 15–30 detectable events per year, with 7 to 15 (2 to 5) being BH–BH (BH–NS) mergers. Other merger scenarios for BH binaries in galactic nuclei exist (e.g., Bartos et al. 2017; Stone et al. 2017); however, future observations by LISA should be able to distinguish between them (Hoang et al. 2019).

There will also be a small number of neutron stars with WD companions, which can evolve into ultracompact X-ray binaries (e.g., Bobrick et al. 2017). Some of these systems will also have been low-mass X-ray binary (LMXB) or transient X-ray source (Zhu et al. 2018) candidates before the secondaries became WDs, potentially explaining part of the observed GC population of X-ray sources (e.g., Hailey et al. 2018; for examples of LMXB formation models, see Naoz et al. 2016; Generozov et al. 2018).

The dynamical and evolutionary outcomes of our simulations listed above are summarized in Figure 3.

4. Conclusions

We have followed the dynamical evolution of binary stars in the vicinity of an SMBH following a burst of star formation, including the effects of stellar evolution, tides, and GR. In the first few megayears, about 25% of binaries became unbound due to scattering interactions with passing stars, while 10% merged due to EKL-induced high eccentricities, 2% crossed their companion's Roche lobe due to stellar expansion, and 13% became tightly bound binaries due to tidal dissipation. Over the next few gigayears, the fraction of unbound binaries rose to 75%, becoming part of the rather mundane population of GC single stars, while the merged and tightly bound binaries evolved into a number of more exotic outcomes. These outcomes include G2-like objects shrouded by gas and dust for an extended period of time, white dwarfs with main-sequence and red giant star companions forming CVs and SBs, some SNe Ia from WD–WD pairs, as well as Type Ia-like events from the collision of red giant helium cores. Furthermore, some compact object binaries form that could be detected as gravitational wave sources. The results are summarized in Figure 3.

These results, of course, can be extended to more continuous or episodic star formation histories, leading to the continuous formation of such binary merger products. If this is the case, we estimate that SN Ia detecting surveys such as ASAS-SN and ZTF would see about 7.5–15 SN Ia, on average, per year from the processes described in this work, out to redshift 0.06. Furthermore, this study suggests that compact object binaries can form at a rate of about $10–20\,\mathrm{yr}^{-1}\,\mathrm{Gpc}^{-3}$, which should yield about 15–30 gravitational wave inspiral events per year detectable by Advanced LIGO, with 7 to 15 (2 to 5) being BH–BH (BH–NS) mergers.

S.N. thanks the KECK Foundation for its partial support of the NStarOrbits Project. S.N. acknowledges the partial support of NASA grant No. 80NSSC19K0321 and also thanks Howard and Astrid Preston for their generous support. S.N. and A.P.S. also acknowledge partial support from the NSF through grant No. AST-1739160. Calculations for this project were performed on the UCLA cluster *Hoffman2*. We thank Vicky Kalogera for facilitating the involvement of `COSMIC` team members in this work and for useful discussions in updating the `BSE` version used in `COSMIC`. We thank the anonymous reviewer for suggestions to improve this paper.

ORCID iDs

Alexander P. Stephan https://orcid.org/0000-0001-8220-0548
Smadar Naoz https://orcid.org/0000-0002-9802-9279
Andrea M. Ghez https://orcid.org/0000-0003-3230-5055
Mark R. Morris https://orcid.org/0000-0002-6753-2066
Katelyn Breivik https://orcid.org/0000-0001-5228-6598
Carl L. Rodriguez https://orcid.org/0000-0003-4175-8881

References

Abbott, B. P., Abbott, R., Abbott, T. D., et al. 2018, LRR, 21, 3
Alexander, T. 2005, PhR, 419, 65
Alexander, T., & Pfuhl, O. 2014, ApJ, 780, 148
Antonini, F., Faber, J., Gualandris, A., & Merritt, D. 2010, ApJ, 713, 90
Antonini, F., Lombardi, J. C., Jr., & Merritt, D. 2011, ApJ, 731, 128
Antonini, F., & Perets, H. B. 2012, ApJ, 757, 27
Bartos, I., Kocsis, B., Haiman, Z., & Márka, S. 2017, ApJ, 835, 165
Belczynski, K., Bulik, T., Fryer, C. L., et al. 2010, ApJ, 714, 1217
Bellm, E. C., Kulkarni, S. R., Graham, M. J., et al. 2019, PASP, 131, 018002
Binney, J., & Tremaine, S. 1987, Galactic Dynamics (Princeton, NJ: Princeton Univ. Press)
Bobrick, A., Davies, M. B., & Church, R. P. 2017, MNRAS, 467, 3556
Bortolas, E., Mapelli, M., & Spera, M. 2017, MNRAS, 469, 1510
Cheng, Z., Li, Z., Xu, X., & Li, X. 2018, ApJ, 858, 33
Chu, D. S., Do, T., Hees, A., et al. 2018, ApJ, 854, 12
Claeys, J. S. W., Pols, O. R., Izzard, R. G., Vink, J., & Verbunt, F. W. M. 2014, A&A, 563, A83
Conselice, C. J., Blackburne, J. A., & Papovich, C. 2005, ApJ, 620, 564
Duquennoy, A., & Mayor, M. 1991, A&A, 248, 485
Fragione, G. 2019, arXiv:1903.03117
Fryer, C. L., Belczynski, K., Wiktorowicz, G., et al. 2012, ApJ, 749, 91
Fryer, C. L., & Kalogera, V. 2001, ApJ, 554, 548
Geller, A. M., Hurley, J. R., & Mathieu, R. D. 2011, BAAS, 43, 327.02
Generozov, A., Stone, N. C., Metzger, B. D., & Ostriker, J. P. 2018, MNRAS, 478, 4030
Genzel, R., Schödel, R., Ott, T., et al. 2003, ApJ, 594, 812
Ghez, A. M., Becklin, E., Duchjne, G., et al. 2003, ANS, 324, 527
Ghez, A. M., Salim, S., Hornstein, S. D., et al. 2005, ApJ, 620, 744
Ghez, A. M., Salim, S., Weinberg, N. N., et al. 2008, ApJ, 689, 1044
Gillessen, S., Eisenhauer, F., Trippe, S., et al. 2009, ApJ, 692, 1075
Gillessen, S., Genzel, R., Fritz, T. K., et al. 2012, Natur, 481, 51
Ginsburg, I., & Loeb, A. 2007, MNRAS, 376, 492
Hailey, C. J., Mori, K., Bauer, F. E., et al. 2018, Natur, 556, 70
Hamers, A. S., Bar-Or, B., Petrovich, C., & Antonini, F. 2018, ApJ, 865, 2
Hees, A., Do, T., Ghez, A. M., et al. 2017, PhRvL, 118, 211101
Heinke, C. O., Ruiter, A. J., Muno, M. P., & Belczynski, K. 2008, in AIP Conf. Ser. 1010, A Population Explosion: The Nature & Evolution of X-ray Binaries in Diverse Environments, ed. R. M. Bandyopadhyay et al. (Melville, NY: AIP), 136
Hoang, B.-M., Naoz, S., Kocsis, B., Farr, W., & McIver, J. 2019, ApJ, 875, 31

Hoang, B.-M., Naoz, S., Kocsis, B., Rasio, F. A., & Dosopoulou, F. 2018, ApJ, 856, 140
Hobbs, G., Lorimer, D. R., Lyne, A. G., & Kramer, M. 2005, MNRAS, 360, 974
Holoien, T. W.-S., Brown, J. S., Vallely, P. J., et al. 2019, MNRAS, 484, 1899
Hopman, C. 2009, ApJ, 700, 1933
Hopman, C., & Alexander, T. 2006, ApJ, 645, 1152
Hurley, J. R., Pols, O. R., & Tout, C. A. 2000, MNRAS, 315, 543
Hurley, J. R., Tout, C. A., & Pols, O. R. 2002, MNRAS, 329, 897
Iben, I., Jr., Tutukov, A. V., & Yungelson, L. R. 1996, ApJ, 456, 750
Izzard, R. G., Jeffery, C. S., & Lattanzio, J. 2007, A&A, 470, 661
Jeans, J. H. 1919, MNRAS, 79, 408
Kamiński, T., Steffen, W., Tylenda, R., et al. 2018, A&A, 617, A129
Kasliwal, M. M. 2012, PASA, 29, 482
Katz, B., & Dong, S. 2012, arXiv:1211.4584
Kiel, P. D., Hurley, J. R., Bailes, M., & Murray, J. R. 2008, MNRAS, 388, 393
Lu, C. X., & Naoz, S. 2019, MNRAS, 484, 1506
Lu, J. R., Do, T., Ghez, A. M., et al. 2013, ApJ, 764, 155
Muno, M. P., Bauer, F. E., Baganoff, F. K., et al. 2009, ApJS, 181, 110
Muno, M. P., Bauer, F. E., Bandyopadhyay, R. M., & Wang, Q. D. 2006, ApJS, 165, 173
Muno, M. P., Lu, J. R., Baganoff, F. K., et al. 2005, ApJ, 633, 228
Naoz, S. 2016, ARA&A, 54, 441
Naoz, S., & Fabrycky, D. C. 2014, ApJ, 793, 137
Naoz, S., Fragos, T., Geller, A., Stephan, A. P., & Rasio, F. A. 2016, ApJL, 822, L24
Nicholls, C. P., Melis, C., Soszyński, I., et al. 2013, MNRAS, 431, L33
Perets, H. B., & Fabrycky, D. C. 2009, ApJ, 697, 1048
Petrovich, C., & Muñoz, D. J. 2017, ApJ, 834, 116
Prodan, S., Antonini, F., & Perets, H. B. 2015, ApJ, 799, 118
Raghavan, D., McAlister, H. A., Henry, T. J., et al. 2010, ApJS, 190, 1
Salpeter, E. E. 1955, ApJ, 121, 161
Schödel, R., Ott, T., Genzel, R., et al. 2003, ApJ, 596, 1015
Sepinsky, J. F., Willems, B., & Kalogera, V. 2007a, ApJ, 660, 1624
Sepinsky, J. F., Willems, B., Kalogera, V., & Rasio, F. A. 2007b, ApJ, 667, 1170
Sepinsky, J. F., Willems, B., Kalogera, V., & Rasio, F. A. 2010, ApJ, 724, 546
Shappee, B. J., & Thompson, T. A. 2013, ApJ, 766, 64
Stephan, A. P., Naoz, S., & Gaudi, B. S. 2018, AJ, 156, 128
Stephan, A. P., Naoz, S., Ghez, A. M., et al. 2016, MNRAS, 460, 3494
Stephan, A. P., Naoz, S., & Zuckerman, B. 2017, ApJL, 844, L16
Stone, N. C., Metzger, B. D., & Haiman, Z. 2017, MNRAS, 464, 946
Taam, R. E., & Ricker, P. M. 2010, NewAR, 54, 65
Toonen, S., Hollands, M., Gaensicke, B. T., & Boekholt, T. 2017, A&A, 602, 16
Trani, A. A., Fujii, M. S., & Spera, M. 2019, ApJ, 875, 42
Tylenda, R., Hajduk, M., Kamiński, T., et al. 2011a, A&A, 528, A114
Tylenda, R., Kamiński, T., Schmidt, M., Kurtev, R., & Tomov, T. 2011b, A&A, 532, A138
Tylenda, R., Kamiński, T., Udalski, A., et al. 2013, A&A, 555, A16
Vink, J. S., & de Koter, A. 2005, A&A, 442, 587
Vink, J. S., de Koter, A., & Lamers, H. J. G. L. M. 2001, A&A, 369, 574
Witzel, G., Ghez, A. M., Morris, M. R., et al. 2014, ApJL, 796, L8
Witzel, G., Sitarski, B. N., Ghez, A. M., et al. 2017, ApJ, 847, 80
Zhang, X., & Jeffery, C. S. 2013, MNRAS, 430, 2113
Zhu, Z., Li, Z., & Morris, M. R. 2018, ApJS, 235, 26